Local Concentration of Folate Binding Protein GP38 in Sections of Human Ovarian Carcinoma by In Vitro Quantitative Autoradiography

Pei Yong Li, Silvana Del Vecchio, Rosa Fonti, Maria V. Carriero, Maria I. Potena, Gerardo Botti, Silvia Miotti, Secondo Lastoria, Sylvie Menard, Maria I. Colnaghi and Marco Salvatore

National Cancer Institute, CNR Nuclear Medicine Center and University Federico II, Naples; and Experimental Oncology E, National Cancer Institute, Milan, Italy

Folate binding protein (FBP) GP38 is a membrane-associated glycoprotein that mediates the intracellular transport of folates. The enhanced expression of FBP in ovarian carcinomas provided a rational basis for clinical studies with specific monoclonal antibodies and some newly synthesized antifolate drugs. Because the outcome of these clinical studies ultimately depends on the degree of FBP expression, we measured the local concentration of FBP using ^{125}I-MOv18 monoclonal antibody and quantitative autoradiography. **Methods:** Tissue sections from 37 specimens of ovarian carcinoma and 13 nonmalignant ovaries were incubated with increasing concentrations of ^{125}I-MOv18 with and without an excess of unlabeled antibody. Tissue-bound radioactivity was measured by quantitative autoradiography. **Results:** Folate binding protein was found to be overexpressed in 91% of nonmucinous ovarian carcinomas, with local concentrations ranging between 1.14 and 82.84 pmole/g. Adjacent tumor sections simultaneously studied with ^{125}I-MOv18 and a ^{125}I-labeled folic acid derivative showed matching and superimposable regional distributions of bound radioactivity of the two radioligands, indicating that the antigen, specifically recognized by ^{125}I-MOv18 in nonmucinous ovarian carcinomas, is capable of binding folates. Nonmalignant ovaries did not contain measurable amounts of antigen when assayed with ^{125}MOv18 but showed a limited and specific binding of the ^{125}I-folic acid derivative to tissue sections. The autoradiographic findings were confirmed by testing sections from mixtures of antigen-positive and antigen-negative cells, by immunoperoxidase staining with MOv18 on tumor sections and by biochemical identification of FBP in membrane fractions from tissue samples. **Conclusion:** Folate binding protein is overexpressed up to 80–90-fold in nonmucinous ovarian carcinomas compared with nonmalignant ovaries. Quantitation of FBP may provide a useful tool in the design of clinical studies with specific monoclonal antibodies and certain antifolate drugs that enter the cell through FBP.

Key Words: folate binding protein; folate receptor; GP38; MOv18; ovarian carcinoma

J Nucl Med 1996; 37:665–672

Folate binding protein (FBP) GP38 is a glycosyl-phosphatidylinositol-linked membrane glycoprotein that mediates the intracellular transport of folate (*1–3*). Two structurally unrelated transport systems are reported to be involved in cellular uptake of folates: (a) a reduced-folate carrier-mediated transport system with transport constant in the micromolar range and (b) a high-affinity FBP with specificity for binding of oxidized folates in the nanomolar range (reviewed in Antony [*1*]). Several malignant cell lines have been reported to express significantly more high-affinity FBP than normal epithelial cells or fibroblasts (*4*), and this expression appears to be modulated by internal and external folate levels (*5,6*).

Recently, Miotti et al. (*7*) developed a monoclonal antibody, MOv18, that recognizes a glycosyl-phosphatidylinositol-anchored M_r 38,000 glycoprotein overexpressed in human nonmucinous ovarian carcinoma. Purification of the antigen and isolation of a complementary DNA sequence encoding the protein led to its identification as a high-affinity FBP (*8,9*). Using immunohistochemical detection methods, MOv18 was shown to be reactive with the vast majority of nonmucinous ovarian carcinomas, whereas no reactivity was observed in normal ovary epithelium, uterus and vagina (*7,10*). A limited expression of the antigen was also found in normal adult kidney tubules and more abundantly in oviduct epithelium (*10,11*). By using another monoclonal antibody, MOv19, reacting against a different epitope on the same FBP, the localization study was extended to a number of normal and malignant human tissues, and a slight reactivity was observed on the granulosa cells of the ovary and in the uterus (*4,12*). Although FBP distribution has been extensively studied, and most investigators have agreed on the limited expression in normal tissues and selective overexpression in nonmucinous ovarian carcinomas, no quantitative data on tissue GP38 concentration are available at present.

The enhanced expression of FBP GP38 in ovarian carcinomas provided a rational basis for in vivo immunotargeting of tumor deposits with both murine (*13*) and chimeric (*14,15*) radiolabeled MOv18. New therapeutic strategies using MOv18 monoclonal antibody have been also tested in preclinical models (*16*) and in patients with ovarian carcinoma (*17*). An additional clinical role of FBP has been highlighted by the recent synthesis of antifolate drugs, such as CB3717 and ICI-198,583, that enter the cell through FBP (*18,19*). These agents have been reported to have antitumor activity both in the preclinical (CB3717, ICI-198,583) and clinical (CB3717) setting (*20–22*).

Because the level of FBP expression in tumor tissues may be predictive of the outcome of clinical studies with specific monoclonal antibodies or with new antifolate drugs, we determined the local concentration of FBP in ovarian carcinomas and nonmalignant ovaries using in vitro quantitative autoradiography. This technique has been extensively used to determine the binding parameters of hormones and neurotransmitters to receptor sites (*23*) and to quantitate tumor-associated antigens in histological sections of solid tumors (*24*). In the present study we used the same technique and ^{125}I-labeled MOv18 to assess the degree of FBP expression in histological sections of ovarian carcinomas and nonmalignant ovaries. Moreover, to test the correspondence between ^{125}I-MOv18 reactivity and folic acid binding, similar studies were performed using a ^{125}I-labeled folic acid derivative.

Received Jan. 10, 1995; revision accepted Oct. 8, 1995.

For correspondence or contact: Silvana Del Vecchio, MD, Medicina Nucleare, II Facoltá di Medicina, Via S. Pansini, 5, 80131 Naples, Italy.

MATERIALS AND METHODS

Monoclonal Antibodies and Radiolabeling

Murine monoclonal antibodies MOv18 and MOv19 recognize different epitopes of the high-affinity FBP (*7–9*) and do not react with the low-affinity folate carrier (*4*). Immunohistochemical characterization of both monoclonal antibodies has been reported in detail elsewhere (*10,11*). In particular, MOv18 showed a strong reactivity with nonmucinous ovarian carcinomas, whereas no significant immunoreaction could be observed in normal ovary (*10*).

The monoclonal antibody MOv18 was radioiodinated with ^{125}I using the Iodogen method (*25*): 2 nmole of protein were reacted with 900 μCi Na^{125}I and 12 μg Iodogen (Pierce, Rockford, IL). After 10 min, the reaction was stopped by the addition of 1 μmole N-acetyltyrosine. The radiolabeled protein was purified from unbound iodide by Sephadex G25 (Pharmacia, Uppsala, Sweden) chromatography. The mean percentage of ^{125}I incorporation was 63%. The protein concentration of the radiolabeled product was determined by the method of Bradford (*26*). The specific activity of the product was 4.29 ± 0.65 μCi/μg (mean ± s.e.m.). Immunoreactivity of the radiolabeled monoclonal antibody was assessed by the method of Lindmo et al. (*27*), and the mean value was 67%.

Tissue Samples and Saturation Study with Iodine-125-MOv18

Twenty-nine patients undergoing surgery for malignant ovarian tumors (26 nonmucinous, 3 mucinous) and 13 patients with nonmalignant disease were studied. A total of 37 specimens of malignant ovarian tumors (34 nonmucinous, 3 mucinous) and 13 nonmalignant ovaries (7 benign lesions, 6 normal tissues) were collected. Tissue samples were immediately frozen in liquid nitrogen after surgical removal and stored at −80°C. Consecutive 8-μm frozen sections were obtained from these specimens, mounted on gelatinized slides and fixed in 0.25% glutaraldehyde. For histological comparison, adjacent sections were stained with hematoxylin and eosin.

The tissue sections used to determine the extent of nonspecific binding were preincubated in a humidity chamber (30 min, 22°C) with a 3.3 μM solution of unlabeled MOv18 and washed for 5 min in cold phosphate-buffered saline (PBS). All sections were then incubated with PBS containing 2% bovine serum albumin (BSA) and 10% chicken serum, washed in PBS and finally incubated with increasing concentrations of ^{125}I-MOv18 (range 0.5–36 nM) for 1 hr at 22°C with and without an excess of unlabeled antibody (0.16 μM). Increasing unlabeled antibody in the incubation medium by a factor of 10 did not cause a significant reduction of the nonspecific binding (*24*). The sections were then washed in cold PBS (30 min) and dehydrated in ethanol.

Tissue Binding of Iodine-125-Folic Acid

To test whether the antigen reacting with ^{125}I-MOv18 can also bind to folates, tissue sections from eight malignant ovarian tumors (tumors 1–8) and seven nonmalignant ovaries (five benign lesions, two normal tissues) were studied using a ^{125}I-labeled folic acid derivative (histamine derivative, [1-carboxy-3-(N)2-(4-[^{125}I]iodo-imidazolyl] ethyl [carbonoyl]-1-pteroyl-amino propane). Tissue sections adjacent to those used in the saturation assay with ^{125}I-MOv18 were first washed in a cold saline solution (0.15 M NaCl, adjusted to pH 3 with glacial acetic acid) for 30 sec to remove endogenously bound folate, neutralized in ice-cold PBS and then incubated for 1 hr at 22°C with 6.9 nM of ^{125}I-folic acid derivative (specific activity 2200 Ci/mmole) in 0.2 M sodium borate, pH 9.4. Nonspecific binding of radioligand to tissue sections was determined using a large excess of unlabeled folic acid (6 μM).

Quantitative Autoradiography

Quantitative autoradiographic techniques and preparation of autoradiographic standards have been previously described (*24*). Briefly, serial dilution of ^{125}I-labeled serum albumin were prepared and added to 20% gelatin. Aliquots of the gelatin suspensions were weighed and counted in a gamma counter. The remainder of each suspension was frozen in liquid nitrogen, and sections were cut from each frozen gelatin stick and used as autoradiographic standards.

The tissue sections, along with the autoradiographic standards, were exposed for 2 days, and the resulting images were digitized using an image analysis system including a high-resolution charged-couple drive and the Micro Computer Imaging Device (Imaging Research, Inc., Ontario, Canada). The absorbance readings over the ^{125}I standards were plotted against the respective microcuries per gram in each standard. A polynomial fitting of these data provided a standard curve. Tumor areas were defined, and regions of interest were drawn over these areas. The mean absorbance values of the selected regions were obtained, and the microcuries per gram of tumor were determined from the standard curve. Using the specific activity of each ^{125}I-MOv18 preparation, the microcuries per gram were converted to picomoles of antibody bound per gram of tissue.

The experimental binding data from each tumor were fitted with the function $TB = (Bmax \times L)/(Kd + L) + aL$, where TB is the total binding of ^{125}I-MOv18 (picomoles per gram); Bmax is the maximal amount of ^{125}I-MOv18 specifically bound to tissue (picomoles per gram); L is the concentration of ^{125}I-MOv18 in the incubation medium (nanomolar); Kd is the dissociation constant of the antigen–antibody reaction (nanomolar); and a is the slope of the unsaturable binding curve. The parameters Bmax and Kd were estimated by the GraphPAD Inplot program (GraphPAD Software, San Diego, CA), which iteratively adjusted their values to obtain the best fit of the data (i.e., minimized the sum of square residuals) and simultaneously provided the respective standard error of the estimate (s.e.e.). The Bmax value, expressed as picomoles per gram of tumor, represented the tissue concentration of antigen.

Embedding of Cultured Tumor Cells

We used the ovarian carcinoma cell line OVCA432, which expresses FBP, and the breast carcinoma cell line MDA-MB-231 which does not bear detectable levels of FBP.

Cells were harvested and washed twice in ice-cold PBS. Tumor cells in suspension (5×10^5/200 μl) were preliminarily assayed for ^{125}I-MOv18 binding in the presence or absence of an excess unlabeled antibody. Maximal binding of ^{125}I-MOv18 to tumor cells was determined by conventional Scatchard analysis. The OVCA432 cell line bound 0.12 pmole of ^{125}I-MOv18/10^6 cells, whereas the MDA-MB-231 cells did not significantly react with the ^{125}I-MOv18 monoclonal antibody.

Increasing concentrations of antigen-positive cells (OVCA432) were mixed with antigen-negative cells (MDA-MB-231) and subjected to low-speed centrifugation. Each cell pellet was included in 20% gelatin and frozen in liquid nitrogen to form cell sticks (*28*). The total cell number per gram was held constant, with the percentage of antigen-positive cells ranging from 0% to 100%. Frozen sections from each cell stick were then cut and processed as for the tissue sections.

Tumor Cell Counting and Immunoperoxidase Staining

To define an index of tumor cell density, the histological sections stained with hematoxylin and eosin were examined using a standard optical microscope interfaced to a computerized image

analysis system. Images were acquired at 400× magnification. Tumor cells were automatically counted in 10–20 fields along the two major axes of the tumor region in the section. Cellularity was expressed as the mean number of tumor cells per field in a section. Tumor cell density could not be evaluated when malignant cells were scattered throughout normal parenchyma or clustered in small tumor foci.

Immunoperoxidase staining was performed with the avidin-biotin-peroxidase complex (ABC) method (*29*) on the first group of specimens studied with quantitative autoradiography as previously described (*10*). Sections from 17 samples of ovarian carcinoma and 7 nonmalignant tissues were stained using MOv18 as the primary antibody at a concentration of 0.7 μg and diaminobenzidine as the chromogen. Specimens containing more than 10% of MOv18-stained cells were considered positive.

Biochemical Identification of FBP

Membrane fractions from samples of nonmucinous ovarian carcinoma, normal ovary and serous cystoadenoma were obtained as described by Weitman et al. (*4*). Briefly, 5 μg of native proteins from each membrane fraction were separated by electrophoresis on a 12.5% polyacrylamide gel under nonreducing conditions and then transferred to polyvinylidene difluoride (PVDF) membrane either directly for immunoblot analysis or after polyacrylamide gel treatment with a buffer containing 10 m*M* Tris-HCl, pH 7.4; 50 m*M* NaCl; 20 m*M* EDTA; 4 *M* urea (*30*) for functional binding assay with the ^{125}I-folic acid derivative. The PVDF membrane for immunoblot analysis was blocked in PBS containing 0.1% Tween 20 (PBS-T), 3% BSA and 10% chicken serum and subsequently incubated with 1 μg/ml each of MOv18 and MOv19 in PBS-T. The immunoreaction was detected using the enhanced chemiluminescence Western blot detection system (Amersham International plc, Little Chalfont, UK) according to the manufacturer's protocol.

Functional binding assay with radioiodinated folic acid derivative was performed by incubating PVDF membrane with 5×10^6 cpm radiolabeled compound (specific activity 2200 Ci/mmole) in 3 ml 0.1 *M* sodium borate, pH 9.4. After washing in cold PBS, the membrane was air-dried and autoradiographed at −70°C with intensifying screens.

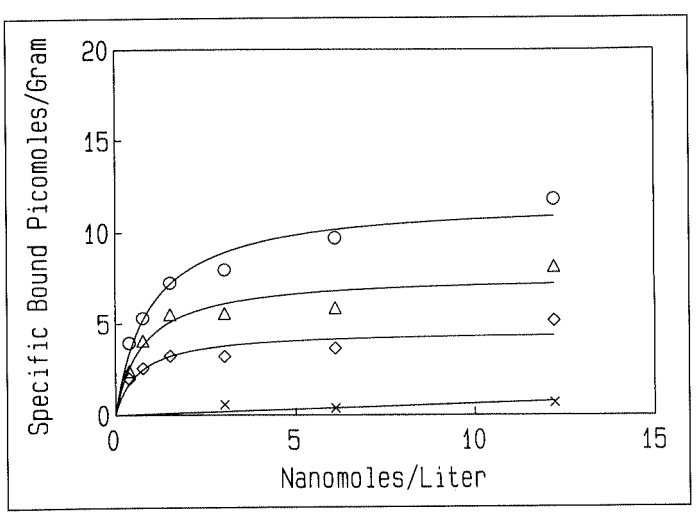

FIGURE 1. Specific binding of ^{125}I-MOv18 to frozen sections of OVCA432 and MDA-MB-231 cells. Antigen-positive (OVCA432, 47×10^6 [○], 83×10^6 [△] and 125×10^6 [○] cells/g) and antigen-negative (MDA-MB-231, 125×10^6 cells/g [×]) cells were mixed and embedded in gelatin. Each cell inclusion contained a fixed total cell number per gram with increasing percentage of positive cells.

TABLE 1
Histologic Findings and Sampling Sites from Patients with Ovarian Carcinoma

Patient no.	Age (yr)	Histologic findings	Tumor no./Site
1	67	Serous	1/Ovary
2	41	Serous	2/Ovary
3	59	Ca. unclass.	3/Ovary
4	44	Endometrioid	4/L. ovary
			5/R. ovary
5	54	Serous	6/Ovary
6	53	Serous	7/Ovary
7	66	Endometrioid	8/Ovary
8	63	Serous	9/L. ovary
			10/R. ovary
			11/Metastasis
9	65	Serous	12/Ovary
10	79	Endometrioid	13/Ovary, internal part
			14/Ovary, middle part
			15/Ovary, external part
11	51	Serous	16/Ovary
12	55	Mucinous	17/Metastasis
13	49	Mucinous	18/Ovary
14	71	Serous	19/Ovary
15	53	Serous	20/Ovary
16	39	Serous	21/Ovary
17	61	Undiff.	22/Ovary
18	52	Serous	23/Ovary
19	61	Serous	24/L. ovary
			25/R. ovary
20	58	Serous	26/Ovary
21	50	Undiff.	27/Metastasis
22	44	Serous	28/L. ovary
			29/R. ovary
23	61	Serous	30/Ovary
24	59	Serous	31/Ovary
			32/Metastasis
25	59	Undiff.	33/Metastasis
26	67	Endometrioid	34/Ovary
27	54	Undiff.	35/Metastasis
28	67	Undiff.	36/Ovary
29	88	Mucinous	37/Metastasis

Undiff. = undifferentiated carcinoma; Ca. unclass. = carcinoma unclassified.

RESULTS

Saturation Study on Cultured Tumor Cells

To establish the optimal experimental conditions for the saturation assay followed by quantitative autoradiography on tissue sections, and to test whether the quantitative autoradiographic measurements were linearly related to antigen concentration, we used mixtures of antigen-positive (OVCA432) and antigen-negative (MDA-MB-231) cells. Frozen sections from gelatin-embedded cells were incubated with increasing concentrations of ^{125}I-MOv18 with and without an excess of unlabeled antibody.

Figure 1 shows the specific binding curves obtained from the saturation assay on cell sections, with the percentage of antigen-positive cells ranging from 0% to 100%. Gelatin-embedded OVCA432 cells bound on average 0.10 pmole of ^{125}I-MOv18/10^6 cells, consistent with the value obtained by Scatchard analysis on cell suspensions. The Bmax values obtained from each cell preparation were significantly correlated to the number of antigen-positive cells per gram ($r = 0.99$; $p < 0.001$). Antigen-negative cells (MDA-MB-231) did not significantly

TABLE 2
Histological Diagnosis of Patients with Nonmalignant Ovaries

Patient no.	Age (yr)	Histologic findings
30	64	Normal ovary
31	47	Normal ovary
32	74	Normal ovary
33	36	Normal ovary
34	28	Normal ovary
35	37	Normal ovary
36	45	Serous cystadenoma
37	42	Serous cystadenoma
38	21	Mucinous cystadenoma
39	57	Fibrotecoma
40	33	Endometriosis
41	18	Cystadenofibroma
42	42	Cystadenofibroma

react with ^{125}I-MOv18, and the binding data best fit a linear function (Fig. 1).

Local Concentration and Distribution of FBP

Tables 1 and 2 report histological diagnosis and sampling sites from patients with ovarian carcinoma and nonmalignant disease, respectively. No patient had received systemic therapy in the 6 mo preceding surgery, except for five (Patients 5, 8, 9, 14 and 20) who had initially undergone a complete course of chemotherapy because of unresectable bulky disease.

Frozen sections from ovarian carcinomas and nonmalignant ovaries were processed in the saturation study with ^{125}I-MOv18, and bound radioactivity was measured by quantitative autoradiography. Figure 2A shows representative binding curves obtained from the assay performed on a nonmucinous ovarian carcinoma (tumor 12). A specific and saturable binding was observed in 31 of 34 (91%) samples from nonmucinous ovarian carcinomas, and the specific binding curves resembled those obtained from the assay performed on sections of antigen-positive cells (Fig. 1). No specific binding of ^{125}I-MOv18 was observed in the remaining malignant tumors (three nonmucinous, three mucinous) and in all nonmalignant tissues, as shown in Figure 2B. In both cases, the binding data best fit a linear function not unlike the assay performed on sections of antigen-negative cells depicted in Figure 1.

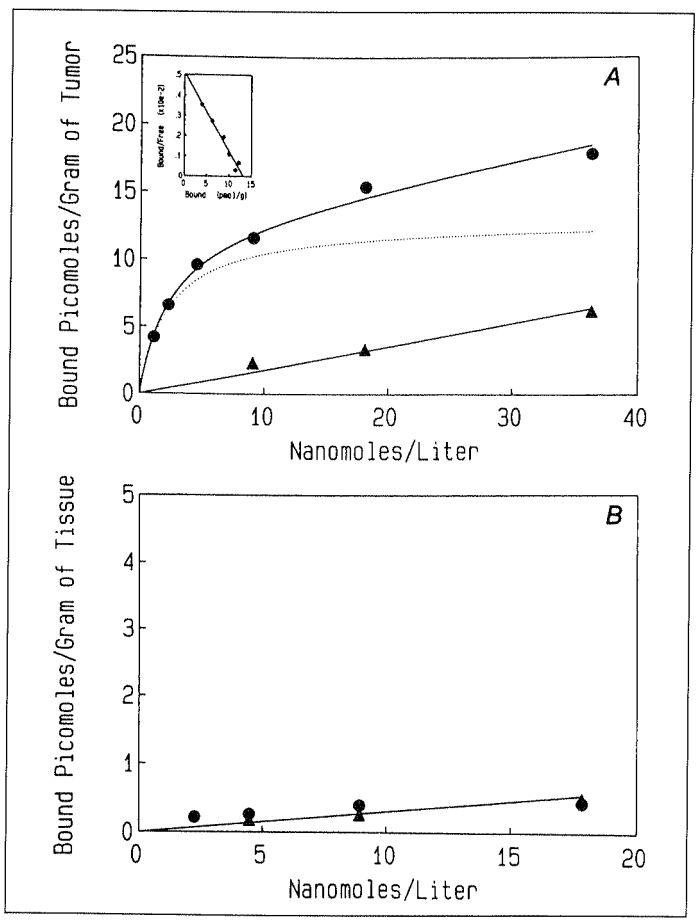

FIGURE 2. Representative binding curves obtained from the saturation assay performed on frozen sections of a nonmucinous ovarian carcinoma (A) and a normal ovary (B). Total binding of ^{125}I-MOv18 (●), nonspecific binding of ^{125}I-MOv18 (▲), specific binding of ^{125}I-MOv18 (· · ·). Inset indicates binding data from panel A were plotted in Scatchard coordinates.

TABLE 3
Results of Saturation Assay with Iodine-125-MOv18 on Sections of Ovarian Carcinomas and Tumor-Cell Density

Tumor no.	Bmax (s.e.e.) (pmole/g)	Kd (s.e.e.) (n*M*)	No. of tumor cells/Field
1	2.20 (0.07)	0.79 (0.14)	95
2	43.46 (3.73)	4.40 (1.06)	117
3	Undet. (—)	Indet. (—)	128
4	82.84 (6.46)	11.02 (1.60)	132
5	27.87 (1.97)	3.71 (0.78)	119
6	21.49 (3.00)	6.17 (2.19)	114
7	70.06 (3.57)	4.40 (0.62)	90
8	1.86 (ND)	8.60 (ND)	Scattered
9	2.00 (0.34)	3.40 (1.59)	Scattered
10	6.97 (1.17)	8.27 (2.85)	Small tumor foci
11	1.14 (0.06)	1.09 (0.23)	Scattered
12	12.83 (0.51)	2.31 (0.37)	96
13	1.36 (0.27)	12.30 (4.58)	134
14	12.60 (1.43)	20.47 (4.70)	127
15	22.70 (1.15)	10.50 (1.32)	131
16	58.32 (8.28)	13.59 (4.47)	140
17	Undet. (—)	Indet. (—)	53
18	Undet. (—)	Indet. (—)	90
19	1.60 (0.82)	11.24 (10.72)	Scattered
20	56.74 (8.05)	31.47 (6.13)	94
21	1.47 (0.17)	8.26 (1.85)	119
22	39.59 (2.96)	8.00 (1.62)	126
23	24.00 (0.93)	4.08 (0.55)	131
24	5.80 (1.76)	5.45 (3.99)	131
25	28.57 (2.19)	8.53 (1.33)	128
26	44.40 (4.08)	3.49 (1.10)	79
27	42.79 (2.86)	10.67 (1.76)	110
28	34.59 (5.88)	13.09 (4.08)	157
29	6.46 (1.34)	8.72 (3.78)	144
30	5.80 (0.64)	8.82 (2.06)	109
31	11.55 (1.01)	2.40 (0.95)	120
32	Undet. (—)	Indet. (—)	Scattered
33	2.88 (0.10)	2.84 (0.37)	86
34	1.86 (0.39)	1.79 (1.42)	117
35	15.50 (1.55)	8.70 (1.81)	142
36	Undet. (—)	Indet. (—)	124
37	Undet. (—)	Indet. (—)	89

Undet. = undetectable; Indet. = indeterminate; ND = not determined (parameters were derived using graphical method).

Table 3 reports the Bmax and Kd values obtained from the saturation assay performed on ovarian carcinomas, along with the respective s.e.e. values. In tumors containing detectable amounts of antigen, Bmax ranged between 1.14 and 82.84 pmole/g (mean ± s.e.m., 22.30 ± 4.07 pmole/g). There was considerable variation in antigen concentration among different specimens, even when they were obtained from the same patient. The lowest antigen expression was observed in a tumor

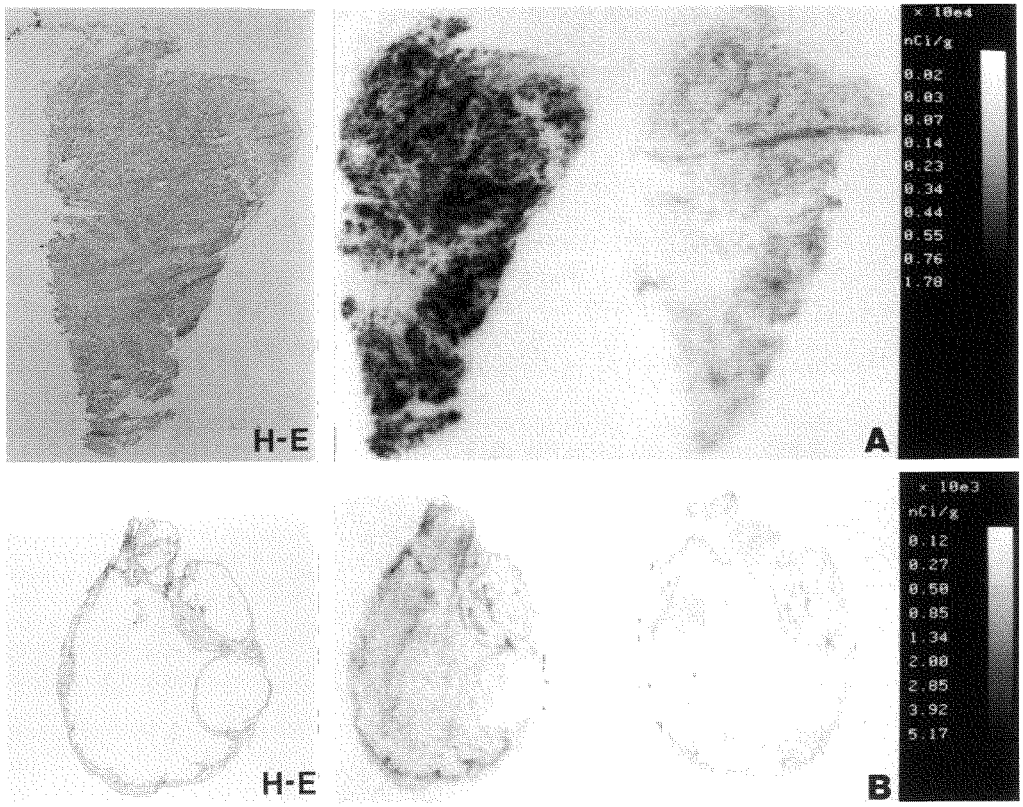

FIGURE 3. Digitized autoradiograms of sections of nonmucinous ovarian carcinoma (A) and nonmalignant ovary (B) incubated with 36 n*M* ^{125}I-MOv18 in the absence (left) or presence (right) of an excess unlabeled antibody. The values of bound radioactivity are shown in the gray scale on the right. H-E = histological sections stained with hematoxylin and eosin.

from a patient (Patient 8) who had undergone chemotherapy before operation and in the internal solid part of a large tumor mass from another patient (Patient 10). Tumor cell density could not account for all the variability observed among ovarian carcinomas because tumors having an equivalent index of cellularity showed a large range of antigen concentration (Table 3). When malignant cells were scattered throughout normal parenchyma, the antigen concentration registered in a large region of interest, including the whole infiltrated tissue, was considerably lower than that measured in the majority of cellularized tumor nodules. Detectable amounts of antigen were also found in four of five metastatic sites of nonmucinous carcinomas.

The mean (±s.e.m.) Kd value was 8.01 ± 1.11 n*M*, consistent with the previously reported Kd value determined by Scatchard analysis on tumor cell lines (*7*). The range of Kd values was approximately fivefold, excluding a few tumors for which Kd values could not be accurately estimated because of a relative lack of data points in the region of Kd or correlation between the two parameters Bmax and Kd in the iterative fitting procedure. The Scatchard plot of each set of binding data was linear (Fig. 2A, inset), indicating a single class of binding sites.

In all cases tested, immunoperoxidase staining confirmed the results obtained by quantitative autoradiography performed on the same samples. In particular, specimens containing measurable amounts of antigen from quantitative autoradiography showed positive staining at immunocytochemical analysis, whereas no chromogenic reaction was observed in quantitative autoradiography of specimens with undetectable amounts of antigen.

Regional distribution analysis of bound radioactivity in tumors containing detectable amounts of antigen showed a heterogeneous pattern of FBP localization (Fig. 3A). By comparing the autoradiograms with the corresponding histological section (hematoxylin-eosin [H-E]), all viable tumor cells appeared to express the antigen, although with variable intensity in different areas of the tumor. Thus, regions of high concentration of FBP were interspersed with areas of low concentration. Tumor areas with a predominant stromal component in the same section showed the lowest ^{125}I-MOv18 binding to tissue. Small clusters of malignant tumor cells interspersed in tumor stroma appeared as focal areas of high radioactivity. For comparison, Figure 3B shows the autoradiographic pattern observed in nonmalignant tissues, where bound radioactivity was lower in intensity, homogeneous in distribution and not displaced by an excess of unlabeled antibody.

Tissue Binding of Iodine-125-Folic Acid

To confirm that the antigen specifically recognized by ^{125}I-MOv18 is capable of binding folates, adjacent sections of nonmucinous ovarian carcinomas were simultaneously studied with ^{125}I-MOv18 and a ^{125}I-labeled folic acid derivative. All malignant tumors showed specific binding of ^{125}I-folic acid derivative. Matching and superimposable regional distributions of bound radioactivity were observed for the two radioligands. Figure 4 shows an example of digitized autoradiographic images obtained from tumor 2 studied with ^{125}I-MOv18 and ^{125}I-folic acid derivative, respectively. Regions of high uptake of ^{125}I-MOv18 coincided with areas of high concentration of bound ^{125}I-folic acid, and both corresponded on the histological section (Fig. 4, H-E) to malignant tumor cells growing in noncontiguous nests or in a packed pattern. Low binding of both radioligands was observed in tumor stroma or necrotic regions. A coincident distribution of binding sites for ^{125}I-MOv18 and ^{125}I-folic acid derivative was assessed for all nonmucinous ovarian carcinomas tested except tumor 3, which did not show specific binding of ^{125}I-MOv18 and presented weak but specific binding of ^{125}I-folic acid derivative.

All nonmalignant ovaries showed limited but specific binding of ^{125}I-folic acid derivative to tissue. In these specimens, the folate binding capacity was considerably lower (up to 89-fold)

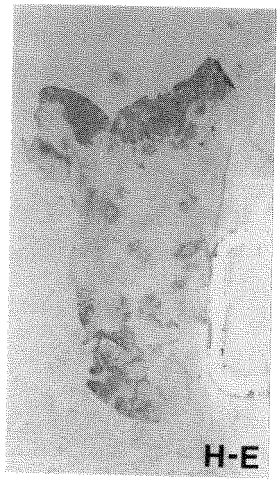

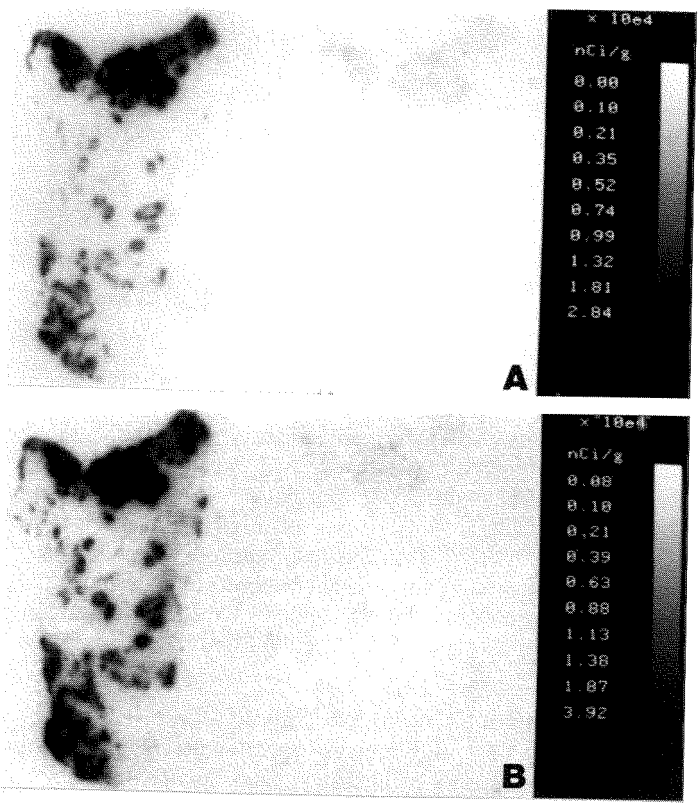

FIGURE 4. Digitized autoradiograms of adjacent sections of a nonmucinous ovarian carcinoma incubated with 36 *nM* ^{125}I-MOv18 (A) and 6.9 *nM* ^{125}I-folic acid derivative (B) in the absence (left) or presence (right) of an excess of unlabeled competitor. The values of bound radioactivity are shown in the gray scale on the right. H-E = histological section stained with hematoxylin and eosin.

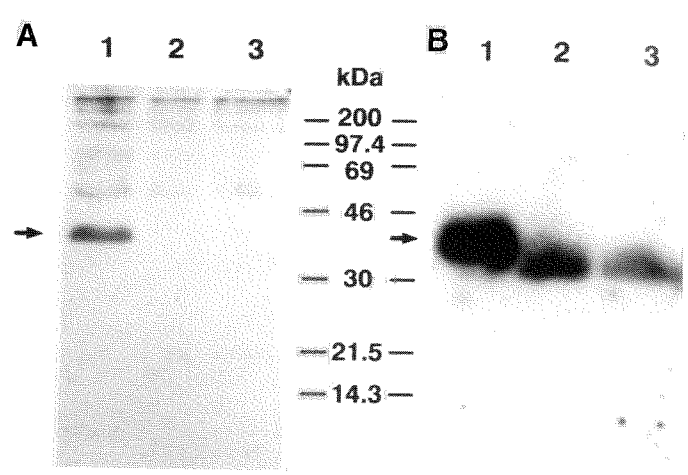

FIGURE 6. Immunoblot analysis (A) and functional binding assay with ^{125}I-folic acid derivative (B) simultaneously performed on membrane fractions from a nonmucinous ovarian carcinoma (lane 1), a normal ovary (lane 2) and a serous cystadenoma (lane 3). Arrow = M_r 38000 protein; ordinate = position of the molecular weight marker proteins; kDa = kilodalton.

than that observed in nonmucinous ovarian carcinomas and showed homogeneous distribution (Fig. 5).

Biochemical Identification of FBP

To test whether a ^{125}I-folic acid derivative actually binds to GP38 in tissue sections, solubilized proteins from membrane fractions of malignant and nonmalignant ovaries were electrophoresed, transferred to PVDF membrane and simultaneously subjected to chemiluminescent immunoblot analysis and functional binding assay with ^{125}I-folic acid derivative.

Incubation of electroblotted proteins with radioiodinated folic acid derivative revealed the presence of a single band of about M_r 38,000 in membrane fractions from a nonmucinous ovarian carcinoma (Fig. 6B, lane 1). A similar band with the same electrophoretic mobility was detected by immunoblot analysis on the same sample (Fig. 6A, lane 1). Lower amounts of FBP were detected by the functional binding assay with ^{125}I-folic acid derivative in membrane fractions of nonmalignant ovaries (Fig. 6B, lanes 2 and 3). Differences in glycosylation or the occurrence of protein isoforms may account for the slightly increased electrophoretic mobility of FBP from nonmalignant tissues with respect to nonmucinous ovarian carcinoma. No signal was obtained from membrane fractions of nonmalignant ovaries by immunoblot analysis (Fig. 6A, lanes 2 and 3).

These findings indicate that the folic acid derivative binds preferentially to a membrane protein exhibiting the same electrophoretic mobility of GP38 as assessed by the immunoblotting technique in nonmucinous ovarian carcinoma. Under these experimental conditions, no other membrane protein with high affinity for folate binding was detected in malignant and nonmalignant ovaries, even with longer exposure.

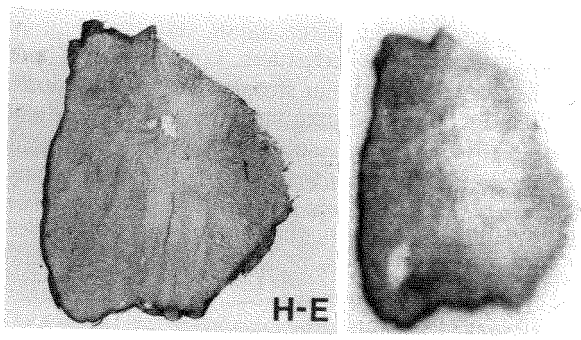

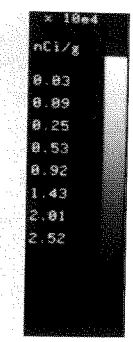

FIGURE 5. Digitized autoradiograms of adjacent sections of a nonmalignant ovary incubated with 6.9 *nM* ^{125}I-folic acid derivative in the absence (left) or presence (right) of an excess unlabeled folic acid (6 μM). The values of bound radioactivity are shown in the gray scale on the right. H-E = histological section stained with hematoxylin and eosin.

DISCUSSION

The present study reports the local concentration and distribution of FBP in 37 specimens of ovarian carcinoma and 13 nonmalignant ovaries using ^{125}I-MOv18 and in vitro quantitative autoradiography. FBP was found to be overexpressed in 91% of nonmucinous ovarian carcinomas, with local concentrations ranging between 1.14 and 82.84 pmole/g, whereas nonmalignant ovaries did not contain measurable amounts of antigen. Functional binding assay with a ^{125}I-labeled folic acid derivative on adjacent tumor sections and on membrane fractions of tissue samples also confirmed the folate binding capability of the antigen specifically recognized by ^{125}I-MOv18 in nonmucinous ovarian carcinomas.

Previous studies have reported in vivo immunotargeting of ovarian carcinoma with both murine (*13*) and chimeric (*15*) radiolabeled MOv18. Those studies showed a specific accretion of radiolabeled MOv18 to tumor lesions, with the achievement of a high tumor-to-nontumor ratio. In particular, the absolute uptake of the chimeric MOv18 registered in cancer deposits 2 and 6 days after intravenous injection of a 1-mg dose was 8.7% and 6.2% injected dose (ID)/kg, respectively, whereas normal tissues contained 2.3% and 1.1% ID/kg at corresponding time points. Similar values of absolute uptake have been reported for other antigen–antibody systems (*15*). When the specific uptake of monoclonal antibody in tumor lesions is compared with the mean concentration of antigen in nonmucinous ovarian carcinoma, we can estimate that only 1%–2% of antigen binding sites is targeted by the antibody.* A large body of evidence indicates that many factors, such as antibody dose, tumor vascular supply, capillary permeability and interstitial pressure, concur to determine a heterogeneous intratumoral distribution and an inefficient penetration of antibody from the blood vessels into tumor nodules (*31–35*). Quantitation of antigen in tumor tissue may provide a useful tool for optimizing the experimental design of clinical studies with monoclonal antibodies in an attempt to increase the occupancy of antigen binding sites in vivo. Similarly, clinical studies with novel antifolate drugs may be modeled on the basis of FBP concentration in tumor tissue.

In tumors containing detectable amounts of antigen, a large range of FBP concentrations was found. This variability could be due either to different tumor cell density among specimens or to a large local variation of antigen expression in different areas of the same tumor, which may indicate a relationship between stages in the replication of tumor cells with expression of the FBP. Furthermore, the large spectrum of local concentrations found in nonmucinous ovarian carcinomas (1.14–82.84 pmole/g) appeared to be lower than the folate binding capacity of certain tumor cell lines (1–50 pmole/10^6 cells) determined by in vitro binding assay with radiolabeled folic acid (*4*). In a recent study, Ross et al. (*36*) analyzed mRNA levels for the folate receptor in a number of established cell lines and tissues. They found that many cultured tumor cells derived from ovary, breast, cervix and colon carcinomas express mRNA for the folate receptor at levels comparable to that expressed by ovarian tumors. On the contrary, choriocarcinoma cell lines and KB epidermoid carcinoma cells showed mRNA levels 10 times greater than the highest levels occurring in carcinoma tumor explants and in other carcinoma cell lines. When OVCA432 cells were tested either in suspension or in tissue-like sections, we found Bmax values of ^{125}I-MOv18 comparable to those obtained by in vitro quantitative autoradiography in nonmucinous ovarian carcinomas. In particular, the mean local concentration of FBP in tumor sections was equivalent to the maximal binding of the antibody to 250×10^6 OVCA432 cells.

Quantitative autoradiographic techniques have been developed for both in vivo tracer kinetic evaluation and in vitro receptor binding studies, allowing measurement of the regional distribution and binding parameters of radioactive ligands (*23*). The same method has been proved suitable for quantitation of tumor-associated antigens in sections of human solid tumors (*24*). In the present study, the reliability of autoradiographic measurements was confirmed by testing antigen-positive and antigen-negative cells and by showing that the maximal binding of ^{125}I-MOv18 to cell sections was linearly related to the number of antigen-positive cells per gram of cell inclusion. Furthermore, the experimental variability measured on tissue-like sections of cultured tumor cells does not exceed 20% (*24*).

The distribution of ^{125}I-MOv18 and ^{125}I-folic acid derivative in adjacent tumor sections was coincident, indicating that the antigen specifically recognized by ^{125}I-MOv18 in nonmucinous ovarian carcinomas is able to bind folates. This finding was confirmed by the biochemical identification in a malignant ovarian tumor of a membrane protein of M_r 38,000 exhibiting a high-affinity binding for ^{125}I-folic acid derivative and the same immunological reactivity of GP38.

Interestingly, nonmalignant ovaries showed limited but specific binding of ^{125}I-folic acid derivative to tissue sections, whereas they did not contain measurable amounts of antigen when assayed with ^{125}I-MOv18. The functional binding assay with ^{125}I-folic acid derivative in membrane fractions of the same tissues confirmed the presence of a FBP with a slightly increased electrophoretic mobility with respect to that found in nonmucinous ovarian carcinoma. This difference could be due either to a different extent of glycosylation or to the occurrence of protein isoforms alternatively present in malignant and normal tissues of the same origin. Previous studies have reported the isolation and characterization of highly homologous FBPs that are encoded by distinct but closely related genes and are differentially expressed in several normal and malignant human tissues (*36–39*). In agreement with the autoradiographic results, no signal could be detected by immunoblot analysis on membrane fractions from nonmalignant ovaries. Because a threefold increase in the amount of immunoblotted proteins gave the same results (data not shown), it cannot be excluded that FBP constitutively expressed in nonmalignant tissues is immunologically unrelated to that found in malignant ovaries. Further studies, however, are needed to test whether MOv18 does recognize only one isoform of FBP.

Finally, the approach that we used in the present study, namely the simultaneous analysis of structure and function of a receptor molecule in sections of human solid tumors may be applied to other systems having biologic relevance in tumor growth and progression.

*Because the tumor compartment contains both bound and free antibody, specific uptake of monoclonal antibody in tumor may be estimated by subtracting normal tissue uptake from tumor uptake. The fractional occupancy of the antigen is calculated by converting percent injected dose per kilogram units to picomoles per gram and dividing by the mean value of Bmax obtained from the saturation assay with radiolabeled monoclonal antibody.

ACKNOWLEDGMENTS

This work was supported by the Associazione Italiana Ricerca Cancro (AIRC). We thank R. Knapp, MD, Dana Farber Institute, for the OVCA432 and Maria Teresa Masucci, MD and Paolo Ascierto, MD for their help and suggestions.

REFERENCES

1. Antony AC. The biological chemistry of folate receptors. *Blood* 1992;79:2807–2820.
2. Kamen BA, Wang MT, Streckfuss AJ, Peryea X, Anderson RGW. Delivery of folates

to the cytoplasm of MA104 cells is mediated by a surface membrane receptor that recycles. *J Biol Chem* 1988;263:13602–13609.
3. Luhrs CA, Slomiany BL. A human membrane-associated folate binding protein is anchored by a glycosylphosphatidylinositol tail. *J Biol Chem* 1989;264:21446–21449.
4. Weitman SD, Lark RH, Coney LR, et al. Distribution of the folate receptor GP38 in normal and malignant cell lines and tissues. *Cancer Res* 1992;52:3396–3401.
5. Kamen BA, Capdevila A. Receptor-mediated folate accumulation is regulated by the cellular folate content. *Proc Natl Acad Sci USA* 1986;83:5983–5987.
6. Kane MA, Elwood PC, Portillo RM, et al. Influence of immunoreactive folate-binding proteins of extracellular folate concentration on cultured human cells. *J Clin Invest* 1988;81:1398–1406.
7. Miotti S, Canevari S, Menard S, et al. Characterization of human ovarian carcinoma-associated antigens defined by novel monoclonal antibodies with tumor-restricted specificity. *Int J Cancer* 1987;39:297–303.
8. Coney LR, Tomassetti A, Carayannopoulos L, et al. Cloning of a tumor-associated antigen: MOv18 and MOv19 antibodies recognize a folate binding protein. *Cancer Res* 1991;51:6125–6132.
9. Campbell IG, Jones TA, Foulkes WD, Trowsdale J. Folate binding protein is a marker for ovarian carcinoma. *Cancer Res* 1991;51:5329–5338.
10. Veggian R, Fasolato S, Menard S, et al. Immunohistochemical reactivity of a monoclonal antibody prepared against human ovarian carcinoma on normal and pathological female genital tissues. *Tumori* 1989;75:510–513.
11. Mantovani LT, Miotti S, Menard S, et al. Folate binding protein distribution in normal tissues and biological fluids from ovarian carcinoma patients as detected by the monoclonal antibodies MOv18 and MOv19. *Eur J Cancer* 1994;30:363–369.
12. Weitman SD, Weinberg AG, Coney LR, Zurawski VR, Jennings DS, Kamen BA. Cellular localization of the folate receptor: potential role in drug toxicity and folate homeostasis. *Cancer Res* 1992;52:6708–6711.
13. Crippa F, Buraggi GL, Di Re E, et al. Radioimmunoscintigraphy of ovarian cancer with the MOv18 monoclonal antibody. *Eur J Cancer* 1991;27:724–729.
14. Molthoff CJM, Buist MR, Kenemans P, Pinedo HM, Boven E. Experimental and clinical analysis of the characteristics of a chimeric monoclonal antibody, MOv18, reactive with an ovarian cancer-associated antigen. *J Nucl Med* 1992;33:2000–2005.
15. Buist MR, Kenemans P, den Hollander W, et al. Kinetics and tissue distribution of the radiolabeled chimeric monoclonal antibody MOv18 IgG and $F(ab')_2$ fragments in ovarian carcinoma patients. *Cancer Res* 1993;53:5413–5418.
16. Mezzanzanica D, Garrido MA, Neblock DS, et al. Human T-lymphocytes targeted against an established human ovarian carcinoma with a bispecific $F(ab')_2$ antibody prolong host survival in a murine xenograft model. *Cancer Res* 1991;51:5716–5721.
17. Bolhuis RLH, Lamers CHJ, Goey SH, et al. Adoptive immunotherapy of ovarian carcinoma with BS-MAb-targeted lymphocytes: a multicenter study. *Int J Cancer* 1992;7(suppl):78–81.
18. Jansen G, Schornagel JH, Westerhof GR, Rijksen G, Newell DR, Jackman AL. Multiple membrane transport systems for the uptake of folate based thymidylate synthase inhibitors. *Cancer Res* 1990;50:7544–7548.
19. Westerhof GR, Jansen G, van Emmerik N, et al. Membrane transport of natural folates and antifolate compounds in murine L1210 leukemia cells: role of carrier- and receptor-mediated transport systems. *Cancer Res* 1991;51:5507–5513.
20. Calvert AH, Newell DR, Jackman AL, et al. Recent preclinical and clinical studies with the thymidylate synthase inhibitor N^{10}-propargyl-5,8-dideazafolic acid (CB3717). *Natl Cancer Inst Monogr* 1987;5:213–218.
21. Cantwell BMJ, Macaulay V, Harris AL, et al. Phase II study of the antifolate N^{10}-propargyl-5,8-dideazafolic acid (CB3717) in advanced breast cancer. *Eur J Cancer Clin Oncol* 1988;24:733–736.
22. Jackman AL, Newell DR, Jodrell DI, et al. In vitro and in vivo studies with 2-desamino-2-CH_3-N^{10}-propargyl-5,8-dideazafolate (ICI 198583), an inhibitor of thymidylate synthase. In: Curtius HC, Gishla S, Blau N, eds. *Chemistry and biology of pteridines*. Berlin: Walter de Gruyter & Co.; 1989:1023–1026.
23. Young AB, Frey KA, Agranoff BW. Receptor assay: in vitro and in vivo. In: Phelps M, Mazziotta J, Schelbert H, eds. *Positron emission tomography and autoradiography: principles and applications for the brain and heart*. New York: Raven Press; 1986:73–111.
24. Del Vecchio S, Reynolds JC, Blasberg RG, et al. Measurement of local Mr 97000 and 250000 protein antigen concentration in sections of human melanoma tumor using in vitro quantitative autoradiography. *Cancer Res* 1988;48:5475–5481.
25. Fraker PJ, Speck JC. Protein and cell membrane iodinations with a sparingly soluble chloramide 1,3,4,6 tetrachloro-3 alpha, 6 alpha-diphenylglycouril. *Biochim Biophys Res Commun* 1978;80:849–857.
26. Bradford M. A rapid and sensitive method for the quantitation of microgram quantities of protein utilizing the principle of protein-dye binding. *Anal Biochem* 1976;72:248–254.
27. Lindmo T, Boven E, Cuttitta F, Fedorko J, Bunn PA. Determination of the immunoreactive fraction of radiolabeled monoclonal antibodies by linear extrapolation to binding at infinite antigen excess. *J Immunol Methods* 1984;72:77–89.
28. Del Vecchio S, Stoppelli MP, Carriero MV, et al. Human urokinase receptor concentration in malignant and benign breast tumors by in vitro quantitative autoradiography: comparison with urokinase levels. *Cancer Res* 1993;53:3198–3206.
29. Hsu SM, Raine L, Fanger H. Use of avidin-biotin-peroxidase complex (ABC) in immunoperoxidase techniques: a comparison between ABC and unlabeled antibody (PAP) procedures. *J Histochem Cytochem* 1981;29:577–580.
30. Silva CM, Tully DB, Petch LA, Jewell MC, Cidlowski JA. Application of a protein-blotting procedure to the study of human glucocorticoid receptor interactions with DNA. *Proc Natl Acad Sci USA* 1987;84:1744–1748.
31. Sands H, Jones PL, Shah SA, Palme D, Vessella RL, Gallagher BM. Correlation of vascular permeability and blood flow with monoclonal antibody uptake by human Clouser and renal cell xenografts. *Cancer Res* 1988;48:188–193.
32. Del Vecchio S, Reynolds JC, Carrasquillo JA, et al. Local distribution and concentration of intravenously injected ^{131}I-9.2.27 monoclonal antibody in human malignant melanoma. *Cancer Res* 1989;49:2783–2789.
33. Sung C, Youle RJ, Dedrick RL. Pharmacokinetic analysis of immunotoxin uptake in solid tumors: role of plasma kinetics, capillary permeability, and binding. *Cancer Res* 1990;50:7382–7392.
34. Juweid M, Neumann R, Paik C, et al. Micropharmacology of monoclonal antibodies in solid tumors: direct experimental evidence for a binding site barrier. *Cancer Res* 1992;52:5144–5153.
35. Shockley TR, Lin K, Sung C, et al. A quantitative analysis of tumor specific monoclonal antibody uptake by human melanoma xenografts: effects of antibody immunological properties and tumor antigen expression levels. *Cancer Res* 1992;52:357–366.
36. Ross JF, Chaudhuri PK, Ratnam M. Differential regulation of folate receptor isoforms in normal and malignant tissues in vivo and in established cell lines. *Cancer* 1994;73:2432–2443.
37. Page TS, Owen WC, Price K, Elwood PC. Expression of the human placental folate receptor transcripts is regulated in human tissues. *J Mol Biol* 1993;229:1175–1183.
38. Shen F, Ross JF, Wang X, Ratnam M. Identification of a novel folate receptor, a truncated receptor, and receptor type β in hematopoietic cells: cDNA cloning, expression, immunoreactivity, and tissue specificity. *Biochemistry* 1994;33:1209–1215.
39. Sadasivan E, da Costa M, Rothenberg SP, Brink L. Purification, properties, and immunological characterization of folate-binding proteins from human leukemia cells. *Biochim Biophys Acta* 1987;925:36–47.